CHEMISTRY
A EUROPEAN JOURNAL

ChemPubSoc
Europe

DOI: 10.1002/chem.201300377

Diastereoselective Hydrogen-Transfer Reactions: An Experimental and DFT Study

François Godin,[a, b] Michel Prévost,[a, b] Serge I. Gorelsky,[c] Philippe Mochirian,[a, b] Maud Nguyen,[a, b] Frédérick Viens,[a, b] and Yvan Guindon*[a, b]

Abstract: Radical reductions of halogenated precursors bearing a heterocycle *exo* (α) to the carbon-centered radical proceed with enhanced *anti*-selectivity, a phenomenon that we termed "exocyclic effect". New experimental data and DFT calculations at the BHandHLYP/TZVP level demonstrate that the origin of the exocyclic effect is linked to the strain energy required for a radical intermediate to reach its reactive conformation at the transition state ($\Delta E^{\neq}_{strain}$). Furthermore, radical reductions of constrained THP systems indicate that high 2,3-*anti* inductions are reached only when the radical chain occupies an equatorial orientation. Hydride deliveries to different acyclic substrates and calculations also suggest that the higher *anti*-selectivities obtained with borinate intermediates are not related to the formation of a complex mimicking an exocycle. From a broader standpoint, this study reveals important conformational factors for reactions taking place at a center vicinal to a heterocycle or an α-alkoxy group.

Keywords: borinate · conformational analysis · density-functional calculations · diastereoselectivity · radical reactions

Introduction

Creating stereogenic centers using free-radical intermediates has been a topic of great interest.[1–3] Our group contributed to this field[4] by developing efficient stereoselective tandem strategies involving radical reactions with anionic processes that allowed the efficient synthesis of complex fragments of biologically relevant ionophores,[5] such as zincophorin (**1a**)[6] or narasin (**1b**)[7] (Figure 1).

The strategies that we have developed involved carbon-center radicals (generated from a mixture of halogenated precursors, such as **2a**,**b** and **4a**,**b**) flanked on one side by an ester and, on the other, by a stereogenic center bearing an electron-withdrawing group. Substrates with a C–O bond at C3 embedded in a ring were reduced with higher selectivities than comparable acyclic substrates having a small alkyl group at that position [Eq. (1) vs. Eq. (2)].[8]

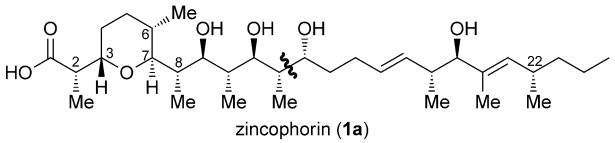

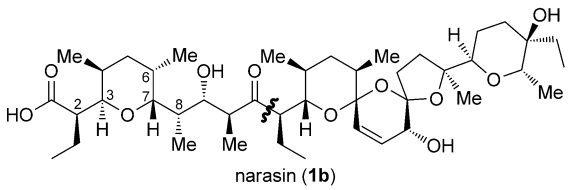

Figure 1. Structure of zincophorin (**1a**) and narasin (**1b**).

This magnification of selectivity with cyclic systems was therefore termed the *exocyclic effect*. Taking advantage of this effect allowed for the reliable synthesis of 2,3-*anti* propi-

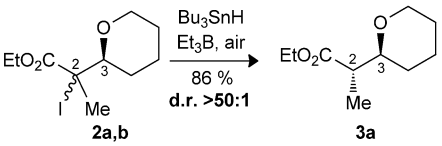

(1)

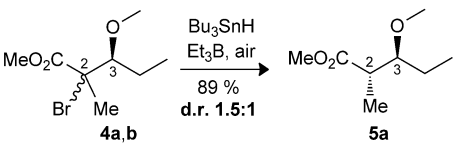

(2)

[a] F. Godin, Dr. M. Prévost, Dr. P. Mochirian, M. Nguyen, F. Viens, Prof. Dr. Y. Guindon
Département de Chimie, Université de Montréal
C.P. 6128, Succursale Centre-Ville, Montréal
Québec, H3C 3J7 (Canada)

[b] F. Godin, Dr. M. Prévost, Dr. P. Mochirian, M. Nguyen, F. Viens, Prof. Dr. Y. Guindon
Bio-organic Chemistry Laboratory
Institut de Recherches Cliniques de Montréal (IRCM)
110 avenue des Pins Ouest, Montréal, Québec, H2W 1R7 (Canada)
Fax: (+1) 514-987-5789
E-mail: yvan.guindon@ircm.qc.ca

[c] Dr. S. I. Gorelsky
Department of Chemistry and Center for
Catalysis Research and Innovation, University of Ottawa
10 Marie Curie, Ottawa, Ontario, K1N 6N5 (Canada)

Supporting information for this article is available on the WWW under http://dx.doi.org/10.1002/chem.201300377.

onate relationships[9] found within numerous ionophores bearing tetrahydropyran (THP) rings or tetrahydrofuran rings (THF).[5,8a–c,e,f]

To overcome the limitations observed with less substituted acyclic compounds, such as **4a**,**b**, we next studied the reduction of C3–C5 diol radical precursors temporarily protected as acetonides or benzylidenes to take advantage of the exocyclic effect [Eq. (3)].[8c] The high 2,3-*anti* inductions obtained then encouraged us to develop single-pot methodologies with boron Lewis acids to form in situ cyclic boronates and borinates [Eq. (4) and Eq. (5)].[4f,8f] Aluminum and magnesium Lewis acids, which were demonstrated to allow the formation of endocyclic radical intermediates by complexation of the ester and the C3–alcohol group, afforded selectively the complementary 2,3-*syn* inductions [Eq. (6)].[4a,f,10] The stereocontrol brought by these radical reduction strategies proved to be highly reliable. By combining them with anionic Mukaiyama aldol reactions, a comprehensive approach to the preparation of polypropionates[4f] was elaborated for the synthesis of all possible 16 polypropionate stereopentads as single diastereoisomers from α-chiral β-hydroxyaldehydes.[4d]

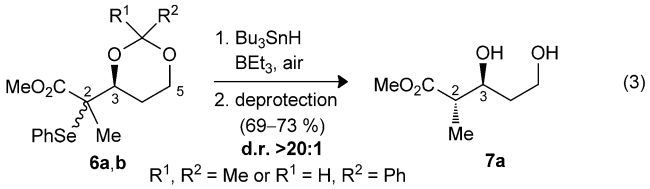

(3)

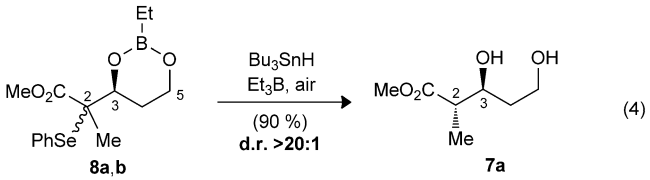

(4)

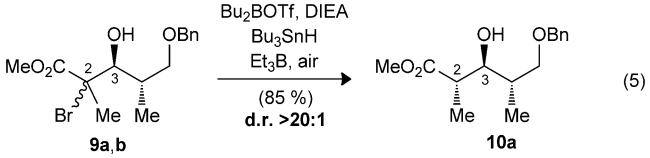

(5)

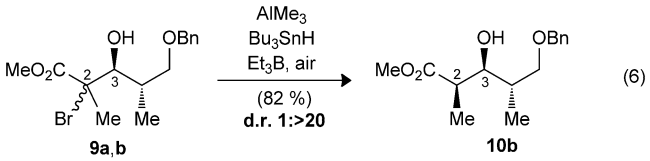

(6)

Reported herein is the first transition state DFT study that investigates the origin of the *anti*-selectivity observed for these types of radical hydrogen-transfer reactions. We were particularly interested in elucidating the factors responsible for the enhanced stereocontrol with substrates bearing an exocycle [Eq. (1) vs. Eq. (2)] or a borinate protecting group [Eq. (5)]. The impact of axial or equatorial orientation of the chain bearing the radical *exo* to a THP was also examined with constrained bicyclic systems. Impressive correlation between the experimental results and theoretical calculations were found and improved our understanding of the reactivity of these radical intermediates. We show that the exocyclic and the borinate effects, which lead to an increase of diastereoselectivity, originate from the alleviation of destabilizing interactions with the incoming hydride in the transition state leading to the major product (2,3-*anti*), whereas the presence of a bulkier side chain at C3 increases the energy of the transition state leading to the minor isomer (2,3-*syn*).

Results and Discussion

The diastereoselectivity enhancement for the radical reduction of systems bearing an exocycle at C3 was first hypothesized to be linked to the conformational biases imposed at the C3–O and C3–C4 bonds (Scheme 1). The chain at C3

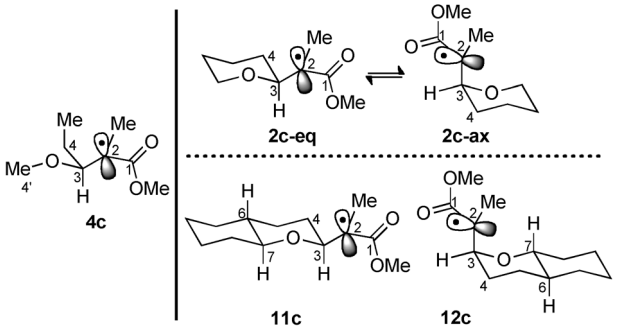

Scheme 1. Acyclic and exocyclic radical intermediates **4c**, **2c**, **11**–**12c** (generated from bromide precursors **4a**,**b**, **2a**,**b** or **11**–**12a**,**b**).

bearing the radical in the exocyclic systems should occupy preferably either equatorial (eq) or axial (ax) positions of low energy chair-like conformations of the THP ring **2c** (Scheme 1).[11] Although it could reasonably be assumed that the equatorial position is preferred for steric factors, we could not rule out completely the possibility that a radical center might prefer to react in the axial position. In order to gain experimental insight on the impact of equatorial or axial orientations of the C3 chain bearing the radical on a THP ring, 6,7-*trans*-octahydrochromen derivatives **11a**;**11b** and **12a**;**12b** were prepared (Scheme 2) and then submitted to hydrogen-transfer reactions with trialkyltin hydride (Table 1).[12]

The reaction sequence to access selectively either the 3,7-*cis* or 3,7-*trans*-6,7-*trans*-octahydrochromen radical precursors is presented in Scheme 2. The olefin **13**, obtained from copper-catalyzed Grignard addition to cyclohexene oxide, was first treated with OsO_4/$NaIO_4$[13] to give the corresponding aldehyde in equilibrium with its lactol isomer. Wittig

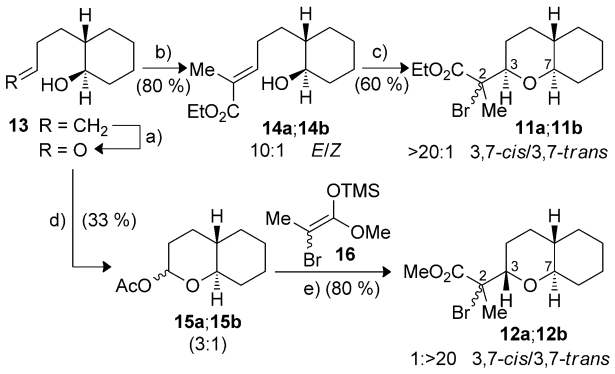

Scheme 2. Synthesis of radical precursors **11a**,**b** and **12a**,**b**. Reaction conditions: a) OsO_4, 2,6-lutidine, $NaIO_4$, 1,4-dioxane/H_2O (3:1), RT; b) $Ph_3PC(Me)=CO_2Et$, CH_2Cl_2, RT; c) NBSac, MeCN, 0 °C to RT; d) Ac_2O, pyridine/CH_2Cl_2 (1:1), 0 °C to RT; e) $SnCl_4$, **16**, CH_2Cl_2, −78 °C.

olefination provided the α,β-unsaturated ester **14a**,**b** (10:1, *E*/*Z*), whereas treatment with acetic anhydride afforded a mixture of the corresponding acetals **15a**,**b** (3:1). The inseparable mixture of **14a**,**b** was then treated with *N*-bromosaccharin (NBSac)[14] to provide a mixture of C2 tertiary bromides **11a**;**11b** with high 3,7-*cis* selectivity. Alternatively, acetals **15a**,**b** were treated with tetrasubstituted enoxysilanes **16** and $SnCl_4$[4e] to afford C2 tertiary bromides **12a**;**12b** with excellent 3,7-*trans* stereocontrol.

Table 1. Radical reductions of 6,7-*trans*-octahydrochromen radical precursors **11a**,**b** and **12a**,**b**.

Entry	R_3SnH	Solvent	d.r. (**a**/**b**)[a]	Yield [%][b]
	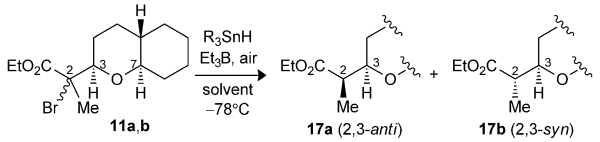			
	11a,**b**		**17a** (2,3-*anti*)	**17b** (2,3-*syn*)
1	Ph_3SnH	PhMe	>20:1	72
2	Bu_3SnH	DCM	>20:1	74
	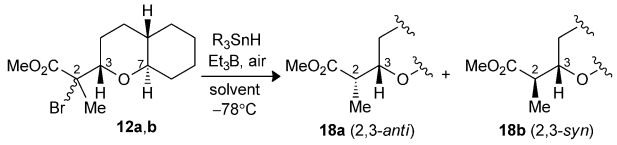			
	12a,**b**		**18a** (2,3-*anti*)	**18b** (2,3-*syn*)
3	Ph_3SnH	PhMe	1.8:1	76
4	Bu_3SnH	DCM	1:5.2	–[c]

[a] Product ratios were determined by ^{1}H NMR analysis of the crude reaction mixture. [b] Yields of isolated products. [c] Complete conversion was observed by ^{1}H NMR spectroscopy.

The radical precursors **11a**,**b** (bearing the C3-chain equatorial) was reduced with an excellent ratio favoring the 2,3-*anti* product **17a** (>20:1), whereas a strikingly poor ratio (1.8:1, **18a**/**18b**) was obtained for substrates **12a**,**b** with the radical-bearing chain forced to occupy an axial orientation (Table 1, entries 1 and 3). It is noteworthy that when performing the reduction with Bu_3SnH in DCM, high 2,3-*anti* selectivity was maintained with equatorial precursors **11a**,**b**, whereas an inversion of selectivity in favor of the 2,3-*syn* products (1:5.2, **18a**/**18b**) was induced from the axial precursors **12a**,**b** (Table 1, entries 2 and 4). The chain bearing the radical equatorial therefore provides higher 2,3-*anti* selectivities than when oriented axially—an intriguing observation that will be further examined in silico.

Description of the computational method: All geometry optimizations were performed using standard gradient techniques and tight SCF convergence in Gaussian 09[15] with the BHandHLYP functional.[16] This functional was demonstrated[17] to be well suited for radical systems.[18] Transition state calculations were performed with Me_3SnH. This hydride led to experimental selectivities comparable to Bu_3SnH (vide infra). The effective core potential of Hay and Wadt[19] LANL2DZ supplemented with a single set of *d*-type polarization functions was used for tin ($d(\zeta)_{Sn}=0.20$),[18b,d,20] together with the valence triple-ζ TZVP basis set[21] for all other atoms. For each reaction, the difference in Gibbs free energies of activation ($\Delta\Delta G^{\ddagger}$) was calculated between the lowest energy *anti*- and *syn*-predictive TS, and the ratio of products was calculated from Equation (7).

$$\Delta\Delta G^{\ddagger} = \mathrm{RT} \times \ln\frac{[2,3\text{-}anti]}{[2,3\text{-}syn]} \qquad (7)$$

To determine Gibbs free energies in solution, geometry optimizations were performed using the IEFPCM implicit solvation model.[22] More details concerning the computational method used are provided in the Experimental Section and in the Supporting Information.

DFT study of THP radical intermediates: The different energy barriers of the radical ground state were evaluated to support the hypothesis that the radical reduction were under Curtin–Hammett conditions.[23] THP radical intermediate **2c** displayed a low ground state conformer with an equatorial radical chain and two possible *E*- and *Z*-enol radicals (**2c-*E*** and **2c-*Z***), resulting from radical delocalization

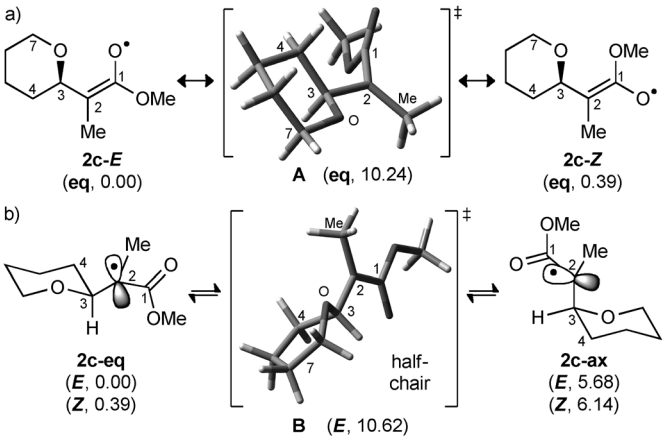

Figure 2. Energy barriers of unsubstituted THP radical **2c**: a) C1−C2 isomerization of *E*-*Z* enol radical, and b) equatorial (eq)–axial (ax) chairs ring flip. Gibbs free energies [kcal mol^{-1}] in toluene are reported relative to the energy of **2c-eq-*E***.

in the ester moiety (Figure 2).[24] Transition state **A** involved in the possible equilibration between these equatorial enol radicals displays a 10.24 kcal mol^{-1} barrier that was determined by the QST3 method in Gaussian (Figure 2).[25] The THP ring flip through half-chair TS **B** was located at 10.62 kcal mol^{-1} for the *E* isomer. These energy barriers are considered to allow ground state equilibration at rates significantly higher than the intermolecular hydride delivery, which occurred with transition state energies greater than 16.3 kcal mol^{-1} at −78 °C.[26]

Transition states analysis of THP intermediates with an equatorial radical chain: C2–C3 Fischer projections of the low energy transition state conformers found for the hydride delivery to radical intermediates are presented at Figure 3.[28] The reported energies in toluene were obtained

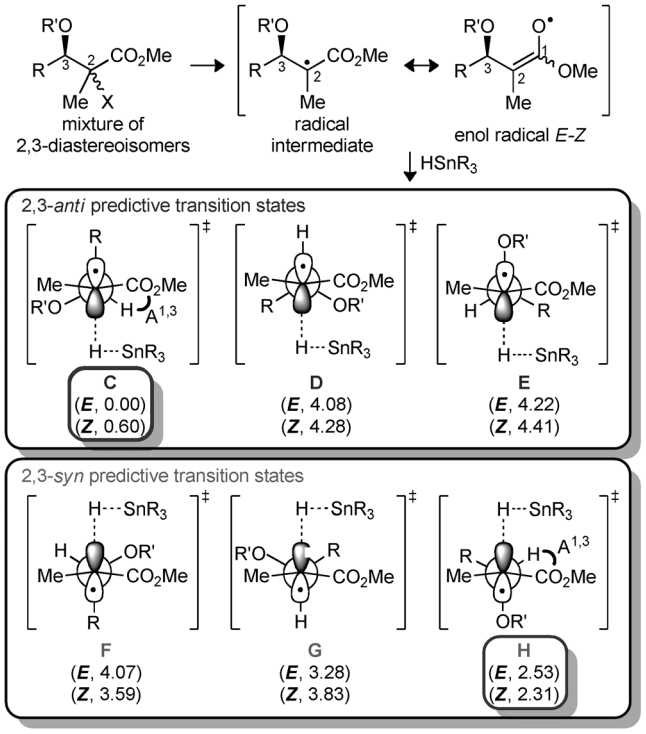

Figure 3. Fischer projections of the C2–C3 conformers of the lowest energy transition states. Gibbs free energies in parentheses [kcal mol^{-1}] in toluene were obtained for the unsubstituted THP radical equatorial **2c-eq** (generated from **2a**,**b**) for the *E* and *Z* isomers and are reported relative to the energy of TS **C-*E***.[27]

for the unsubstituted THP **2c** with the C3-radical chain in the equatorial orientation (R–R′ = −$(CH_2)_4$−). The average C2–H and Sn–H Wiberg bond orders (0.3 and 0.5, respectively) suggest that the reduction occurs in a relatively early TS.[29] Starting from an almost planar conformation (0.6°) at the ground state (**2c-*E*** or **-*Z***, Figure 2), the C3 center of the radical intermediate experiences approximately 10° of pyramidalization[30] at the TS.[31] The allylic-1,3 strain ($A^{1,3}$) minimization observed for the radical intermediate could therefore also represent an important factor to explain why *anti*-predictive TS **C** and *syn*-predictive TS **H** are significantly lower in energy than the other transition states (Figure 3).[28]

The DFT study allowed to confirm that TS **C** would be preferred because of optimal intramolecular dipole–dipole minimization and σ-donation of the C3–C4 bond[24c,32] and revealed the conformation of the lowest *syn*-predictive TS **H**. The presence of more severe allylic-1,2 strain ($A^{1,2}$) in the latter could also account for the lower energy of *anti*-predictive TS **C**. According to the $\Delta\Delta G^{\ddagger}$ calculated between **C-2c-eq**[33] and **H-2c-eq** in toluene (2.31 kcal mol^{-1}) excellent selectivities in favor of the 2,3-*anti* product **2a** are expected at −78 °C (>380:1), which is in agreement with the experimental >50:1 ratio determined by GLC analysis of the crude reaction mixture (Figure 4a).[8a] This $\Delta\Delta G^{\ddagger}$ value also correlates with the calculated and experimental ratios obtained for bicyclic substrate **11c** with the radical chain constrained in the equatorial position, in toluene or DCM (Figure 4b).

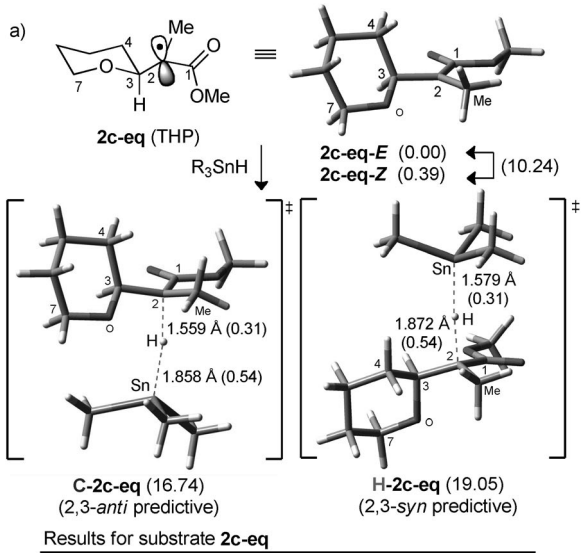

Results for substrate **2c-eq**

conditions at −78°C	ΔΔG‡ (2,3-*anti* **3a**/2,3-*syn* **3b**) exptl[a]	calcd
vacuum	–	**2.39** (>470:1)
toluene	**>1.52** (>50:1)	**2.31** (>380:1)
DCM	–	**1.63** (>60:1)

b) **11c**

Results for substrate **11c**

conditions at −78°C	ΔΔG‡ (2,3-*anti* **13a**/2,3-*syn* **13b**) exptl[a]	calcd
vacuum	–	**1.89** (>120:1)
toluene	**>1.16** (>20:1)	**1.59** (>60:1)
DCM	**>1.16** (>20:1)	**1.22** (>20:1)

[a] Experiments were performed with Bu_3SnH.

Figure 4. Lowest energy transition states of hydride delivery to: a) unsubstituted THP radical **2c-eq**, and b) equatorial bicyclic radical **11c**. Gibbs free energies [kcal mol^{-1}] in toluene are reported in parentheses relative to the energy of **2c-eq-*E***. Atomic distances [Å] and Wiberg bond orders for Sn–H and C2–H interactions are shown for the TS structures.

Transition states analysis of THP intermediates with an axial radical chain: The calculated energies obtained with the bicyclic system **12c**, locking the radical chain in the axial position, correlate well with the poor *anti*-diastereoselectivity obtained in toluene and the reversal of selectivity towards the *syn*-product in DCM (Figure 5).

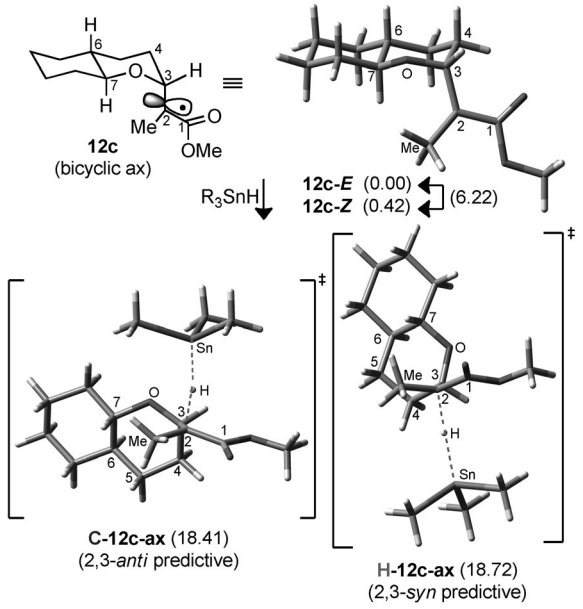

conditions at –78°C	$\Delta\Delta G^{\ddagger}$ (2,3-*anti* **14a**/2,3-*syn* **14b**)	
	exptl[a]	calcd
vacuum	–	**0.73** (6.6:1)
toluene	**0.23** (1.8:1)	**0.31** (2.2:1)
DCM	**–0.64** (1:5.2)	**–0.32** (1:2.3)

[a] Experiments were performed with Bu_3SnH.

Figure 5. Transition states of hydride delivery to axial bicyclic radical **12c**. Gibbs free energies [kcal mol^{-1}] in toluene are reported in parentheses relative to the energy of **2c-ax-*E***.

The analysis of the lowest energy transition states **C** and **H** indicates that the chair conformation is distorted slightly to orient the radical chain (C2–C3) away from the fully axial position (Figure 5). This could alleviate partially two high energy pseudo *syn*-pentane-like interactions (Me–C2–C3–C4–C5 and Me–C2–C3–O–C7) in **C-12c-ax** and one pseudo *syn*-pentane interaction (Me–C2–C3–C4–C5) in **H-12c-ax**. The presence of an additional pseudo *syn*-pentane interaction in **C-12c-ax** should result in a more significant destabilization of the *anti*-predictive TS. The optimal intramolecular dipole minimization in TS **C**, resulting from the antiperiplanar orientation of the ester group (C2–C1) relative to the C3-alkoxy group (C3–O), however, could explain that the 2,3-*anti* product remains preferred in low dielectric media. In a solvent with a higher dielectric constant (e.g., DCM), this stabilization could become less important and increase the relative energy of **C** versus **H**, which would be consistent with the observed reversal to 2,3-*syn* selectivity in DCM for bicyclic compound **12c**. This highlights the importance of considering solvents when studying these radical reactions in silico.[34]

In summary, the analysis of cyclic systems **11c** and **12c** indicated the crucial impact of the conformation (equatorial vs. axial) of the C3-chain bearing the radical to rationalize the increase in diastereoselectivity. We then sought to identify other factors that could explain why acyclic substrates generally lead to a decrease in 2,3-*anti* selectivity [Eq (1) vs. Eq. (2)].

Transition states analysis of acyclic substrate 4c with a secondary C3 side chain: The acyclic radical substrate **4c** was more challenging to analyze because it required the examination of all the possible C1–C2, C2–C3, C3–C4 and C4′–O conformations (Figure 6). All the corresponding rotational energy barriers for **4c** were calculated to be significantly lower than the energy required to reach the transition states, therefore allowing for Curtin–Hammett conditions to be met.[35] In the lowest energy ground state conformation **4c-*E*** (0 kcal mol^{-1}), it is interesting to note that the methoxy group (C4′–O) is pointing downward. This conformation is unlikely to be preferred at the transition state, because severe steric clash would occur with the incoming hydride.[36]

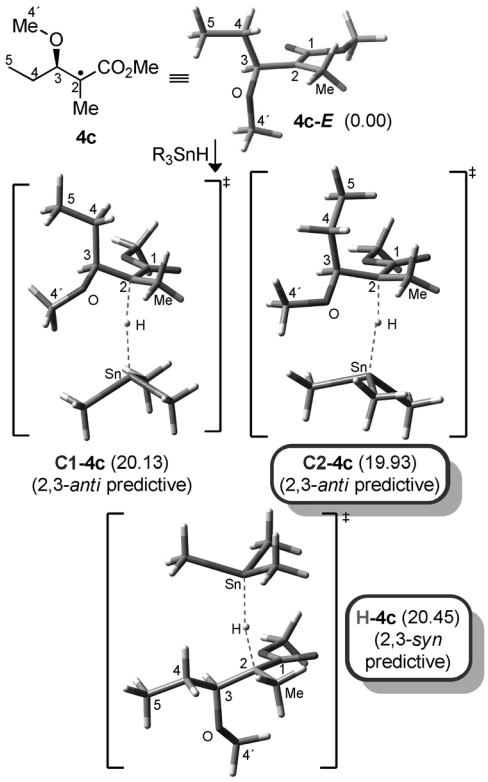

conditions at –78°C	$\Delta\Delta G^{\ddagger}$ (2,3-*anti* **5a**/2,3-*syn* **5b**)	
	exptl[a]	calcd
vacuum	–	**0.38** (2.7:1)
DCM	**0.16** (1.5:1)	**0.52** (3.8:1)

[a] Experiments were performed with Bu_3SnH.

Figure 6. Transition states of acyclic radical intermediate **4c** (from **4a**,**b**) with a methoxy at C3–O. Gibbs free energies [kcal mol^{-1}] in DCM are reported relative to the energy of **4c-*E***.

Indeed, in the lowest energy transition states **C1**-**4c** (20.13 kcal mol^{-1}) and **C2**-**4c** (19.93 kcal mol^{-1}), the C4′–O rotamer adopts a conformation to orient the C4′ away from the hydride reagent. The 0.52 kcal mol^{-1} free energy difference ($\Delta\Delta G^{\neq}$) between the lowest *syn*-predictive TS **H-4c** and **C2**-**4c** in DCM predicts an *anti*-selectivity of 3.8:1 [Eq. (7)] in agreement with the experimental selectivity (1.5:1).

The origin of the exocyclic effect: Acyclic system **4c** adopts a reactive conformation leading to 2,3-*anti* product that presents destabilizing interactions not found in the exocyclic system **2c** (Figures 6 and 4a). This was demonstrated by energy decomposition of the transition state energy ($\Delta E^{\neq}$) using the activation strain model[37,38] ($\Delta E^{\neq} = \Delta E^{\neq}_{strain}[radical] + \Delta E^{\neq}_{strain}[hydride] + \Delta E^{\neq}_{int}$). The interaction energy ($\Delta E^{\neq}_{int}$) and the strain energy ($\Delta E^{\neq}_{strain}$) of the hydride were found to be marginally different in these two systems, which reflects the fact that no severe steric clash with the incoming hydride was found.[35] The strain energy gap of the radical for reaching the *anti*-predictive TS **C** or **C2** (Figure 7), however, is markedly greater in acyclic systems (3.30 vs. 6.30 kcal mol^{-1}; **2c** vs. **4c**), whereas the $\Delta E^{\neq}_{strain}$ in the *syn*-predictive TS **H** for both systems are comparable in energy (5.35 vs. 5.67 kcal mol^{-1}; **2c** vs. **4c**). The additional interaction for radical intermediate **4c** (i.e., C4′ with C4 and C5 with C2) in the lowest *anti*-predictive TS (**C2**), could in part explain this increase in relative energy. Linking C4′ and C5 as an exocycle would provide high 2,3-*anti* inductions by avoiding these unfavorable interactions in the *anti*-predictive TS, which leads to an enhanced $\Delta\Delta G^{\neq}$ gap relative to acyclic intermediate **2c**.

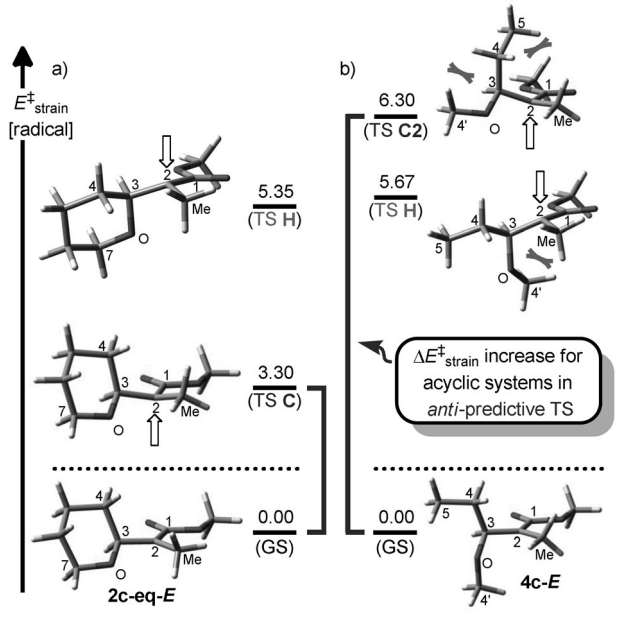

Figure 7. The origin of the exocyclic effect. The $E^{\neq}_{strain}$ energies of the radical [kcal mol^{-1}] are reported relative to the energies of the respective ground state structures of **2c**-**eq**-***E*** and **4c**-***E***. The arrows indicate the trajectory of the incoming hydride for TS **C** or **C2** (*anti*-predictive) and TS **H** (*syn*-predictive).

DFT study of borinate intermediates: Another important aspect of acyclic radical reductions is the impact of installing a borinate at the C3 position of radical intermediate (**I**, Figure 8). These boron intermediates are synthetically more useful than methoxyether groups, since they are convenient to install and to cleave in situ. The high *anti*-selectivity observed for the reduction of borinate intermediates in the context of polypropionate synthesis [R = Me, Figure 8 and Eq. (5)] led us to suggest that a complex (**II**, Figure 8) was mimicking the exocyclic THP [Eq (1)]. The borinate at C3 could also induce the formation of complex **III**, resulting from the intramolecular complexation to the carbonyl of the ester. The hydrogen transfer reaction on such intermediate should, however, lead to the 2,3-*syn* product, as suggested by Equation (6).[39]

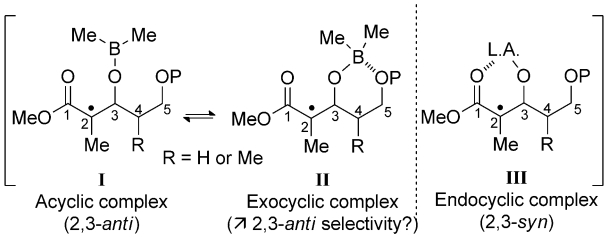

Figure 8. Various complexation modes of C3,C5-alkoxy radical intermediates and resulting outcome (2,3-*anti* or 2,3-*syn*) of hydride transfer reaction.

To determine if the formation of an exocyclic complex was a prerequisite to reach high 2,3-*anti* selectivity, radical precursors **19a**,**b** (R = BBu_2) were prepared and reduced after in situ formation of the corresponding borinate intermediate (Table 2, entry 2). A marginally higher 2,3-*anti* ratio was obtained with the latter, as compared with the corresponding C3-methyl protected **4a**,**b** (4.2:1 vs. 1.5:1, entry 2 vs. 1). Radical precursors **20–23a**,**b** with secondary side chain at C3 and bearing an alkoxy group at C5 were then examined under the standard reducing conditions (Table 2, entries 3–6). The borinate intermediates furnished significantly higher 2,3-*anti* selectivity than their C3-methoxy protected counterparts.

These results were puzzling, since the higher selectivity obtained with C5-benzyloxy suggested the possible involvement of an exocyclic intermediate, but we were reluctant to invoke the complexation of a bulky silyloxy ether group by boron, as these protecting groups are generally reported to prevent complexation.[40] We have, therefore, decided to investigate these questions by the DFT calculations reported herein.

In the presence of a tertiary alkyl group at C3 (Table 2, entry 8), 2,3-*anti* product **32a** was formed selectively from **25a**,**b**, as it was the case with the corresponding C3-methoxy precursor **24a**,**b** (entry 7). The high level of diastereoselectivity for precursors with bulkier alkyl side chain falls beyond the limit of detection, and it is thus not possible to determine if an enhancement is obtained between **24a**,**b**,

Table 2. Radical reductions of acyclic radical precursors **4a**,**b** and **19**–**25a**,**b**.

Entry	R	Solvent	d.r. (**a**/**b**)[a]	Yield [%][b]
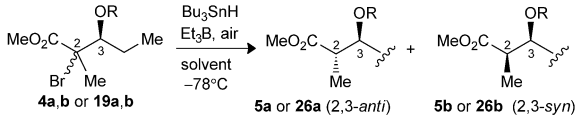 **4a**,**b** or **19a**,**b** → **5a** or **26a** (2,3-*anti*) + **5b** or **26b** (2,3-*syn*)				
1[c] (**4a**,**b**)	Me	DCM	1.5:1 (**5**)	89
2[d] (**19a**,**b**)	BBu_2	DCM	4.2:1 (**26**)	41
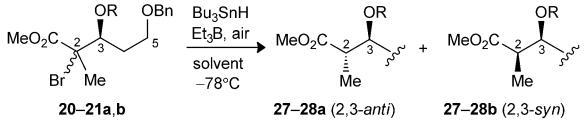 **20**–**21a**,**b** → **27**–**28a** (2,3-*anti*) + **27**–**28b** (2,3-*syn*)				
3 (**20a**)	Me	DCM	1.2:1 (**27**)	75
4[d] (**21a**,**b**)	BBu_2	DCM	9:1 (**28**)	86
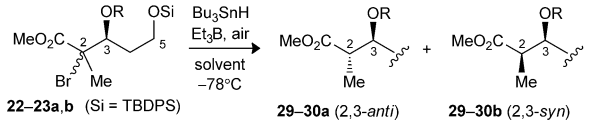 **22**–**23a**,**b** (Si = TBDPS) → **29**–**30a** (2,3-*anti*) + **29**–**30b** (2,3-*syn*)				
5 (**22a**)	Me	DCM	1.4:1 (**29**)	80
6[d] (**23a**,**b**)	BBu_2	DCM	13:1 (**30**)	70
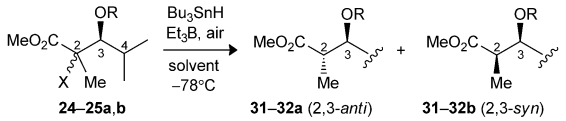 **24**–**25a**,**b** → **31**–**32a** (2,3-*anti*) + **31**–**32b** (2,3-*syn*)				
7[e,f] (**24a**,**b**)	Me	toluene	>20:1 (**31**)	87
8[d,e] (**25a**,**b**)	BEt_2	DCM	>20:1 (**32**)	71

[a] Product ratios were determined by ^{1}H NMR analysis of the crude reaction mixture. [b] Yields of isolated products. [c] Ref. [8c]. [d] Borinate (R = BBu_2 or BEt_2) was generated in situ from secondary alcohol (R = H). The secondary alcohols were isolated (R = H); see the Supporting Information for details. [e] X = Br (entry 7) and X = I (entry 8). [f] Ref. [44].

25a,**b** and **9a**,**b** [Table 2, entries 7–8 and Eq. (5)]. Nevertheless, these results indicate that borinate intermediates are reduced with high *anti*-selectivity through an acyclic mode when a tertiary side chain is present at C3.

The last important point that we explored experimentally is the possibility that borinates provide greater polarization of the C3–O bond by delocalization of oxygen lone pairs in the empty p-orbital of boron. The presence of an electron-withdrawing group at C3 was previously shown to be mandatory for 2,3-*anti* selectivity.[3c,32] Substrates protected with electron-withdrawing groups, such as MOM[41] or trifluoroacetate, were synthesized to examine if they would also increase 2,3-*anti* inductions (Table 3). None of these substrates, however, proceeded with levels of selectivity comparable to the ones obtained with borinates (Table 3, entries 1–3 vs. Table 2, entries 4 and 6). Finally, an erosion of diastereoselectivity was observed when the size of the substituents was increased on the borinate (Table 3, entry 4).

Transition state analysis for the reductions of borinate intermediates: The reduction of the borinate radical intermediate **19c** was analyzed in silico (Figure 9a). The preferred TS (**C-19c**) displays an O–C3–C4–C5 torsion angle similar to the second lowest TS **C1** for methoxy-substituted acyclic intermediate **4c** (Figure 6). The planar trigonal conformation of the borinate likely reduces its interaction with the C5 methyl group in **C-19c**. The bond lengths and conformation obtained by calculations are consistent with the X-ray data obtained from a related borinate compound.[42] The lowest energy transition states **C-19c** and **H-19c** were calculated to have a $\Delta\Delta G^{\ddagger}$ of 0.21 kcal mol^{-1}, which would predict selectivities of 1.7:1, slightly below the experimental value with Bu_3SnH (4.2:1, Table 2, entry 2). Since Me_3SnH[43] was used

Table 3. Radical reductions of radical precursors **33**–**36a**,**b**.

Entry[a]	R	R′	d.r. (**a**/**b**)[b]	Yield [%][c]
 **33**–**36a**,**b** → **37**–**39a**, **28a** + **37**–**39b**, **28b**				
1 (**33a**)	OBn	MOM	1.3:1 (**37**)	87
2 (**34a**)	OTBDPS	MOM	1.5:1 (**38**)	80
3 (**35a**)	OBn	CF_3CO	2.3:1 (**39**)	89
4[d] (**36a**,**b**)	OBn	9-BBN	3:1 (**28**)	82

[a] X = Br (entries 1–3) and X = I (entry 4). [b] Product ratios were determined by ^{1}H NMR analysis of the crude reaction mixture. [c] Yields of isolated products. [d] Borinate (R′ = 9-BBN) was generated in situ from secondary alcohol **21a**,**b** (R′ = H). The secondary alcohols were isolated (R′ = H); see the Supporting Information for details.

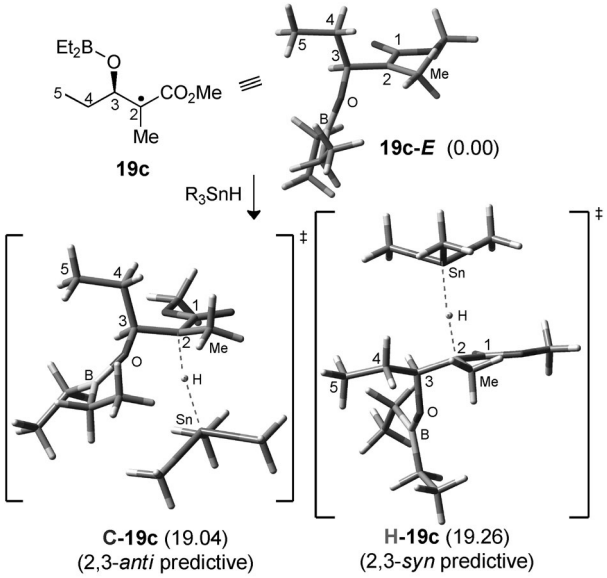

Results for substrate **19c** (borinate Et)

conditions			$\Delta\Delta G^{\ddagger}$ (2,3-*anti* **26a**/2,3-*syn* **26b**)	
hydride	solvent	*T* [°C]	exptl	calcd
Me_3SnH	vacuum	–78	–	**0.24** (1.9:1)
Me_3SnH	DCM	–78	**0.59** (4.6:1)	**0.21** (1.7:1)
Bu_3SnH	DCM	–78	**0.56** (4.2:1)	–
Ph_3SnH	DCM	–78	**0.69** (5.9:1)	–

Figure 9. Transition states of acyclic radical intermediates **19c** (in situ from **19a**,**b**) with a diethylborinate (BEt_2) at C3–O. Gibbs free energies [kcal mol^{-1}] of TS structures in DCM are reported relative to the energy of **19c**-***E***.

in our calculations, we decided to verify experimentally if the hydrogen transfer gave similar results than with Bu_3SnH, which was used throughout this study with acyclic substrates. The reduction of compound **19a**,**b** was also evaluated with Ph_3SnH at −78 °C (Figure 9). The level of *anti*-selectivity obtained with the former (4.6:1) was similar to the ratio Bu_3SnH provided (4.2:1), whereas reduction with the bulkier hydride (Ph_3SnH) led to somewhat higher selectivity (5.9:1, Figure 9). These results suggest that the use of a borinate as a protecting group of the alkoxy group at C3 increases the 2,3-*anti* ratio as compared to corresponding methyl ether. A more extensive in silico evaluation of the borinate effect was, however, necessary to understand this selectivity trend.

Exocyclic complexation versus acyclic reduction of borinate intermediates bearing a C5-alkoxy group: It was observed experimentally that substrates with a secondary side chain at C3 and an alkoxy group at C5 provide higher *anti*-selectivity than the corresponding substrate bearing a C3-ethyl group (Table 2, entry 2 vs. 4). To determine if complexation of the C5-alkoxy was at the origin of this modest, but yet, significant enhancement of selectivity (**II**, Figure 8), transition state calculations were performed with radical **40c** (Figure 10). The *anti*- or *syn*-predictive TS obtained only displayed a weak B−O5 interaction and these structures were not the lowest in energy (**C1** vs. **C2** and **H1** vs. **H2**). Moreover, these calculations indicated that complexation of the boron with the ester (**III**, Figure 8) is likely not involved in the *syn*-predictive TS. The enhancement of *anti*-selectivity with borinates is therefore not linked to the formation of a complex and may result from the particular conformation of these intermediates (Table 2, entries 4 and 6).

Transition state analysis of radical precursors with a tertiary C3 side chain: The transition state analysis performed on **24c** (Figure 11) revealed that the lowest energy *anti*-predictive TS **C-24c** adopts a staggered C4′−O conformation, similar to TS **C1-4c** ($\phi_{C4'\text{-}O\text{-}C3\text{-}H3}$ −1.5°; Figure 6). One could expect that this unfavorable conformation would raise the energy of the *anti*-predictive TS **C**, leading to lower selectivity. The analysis of the lowest energy *syn*-predictive TS **H-24c**, however, indicates that an unfavorable *syn*-pentane-like interactions is present between the C5 and C2-methyl group (Figure 11). The resulting $\Delta\Delta G^{\ddagger}$ value therefore re-

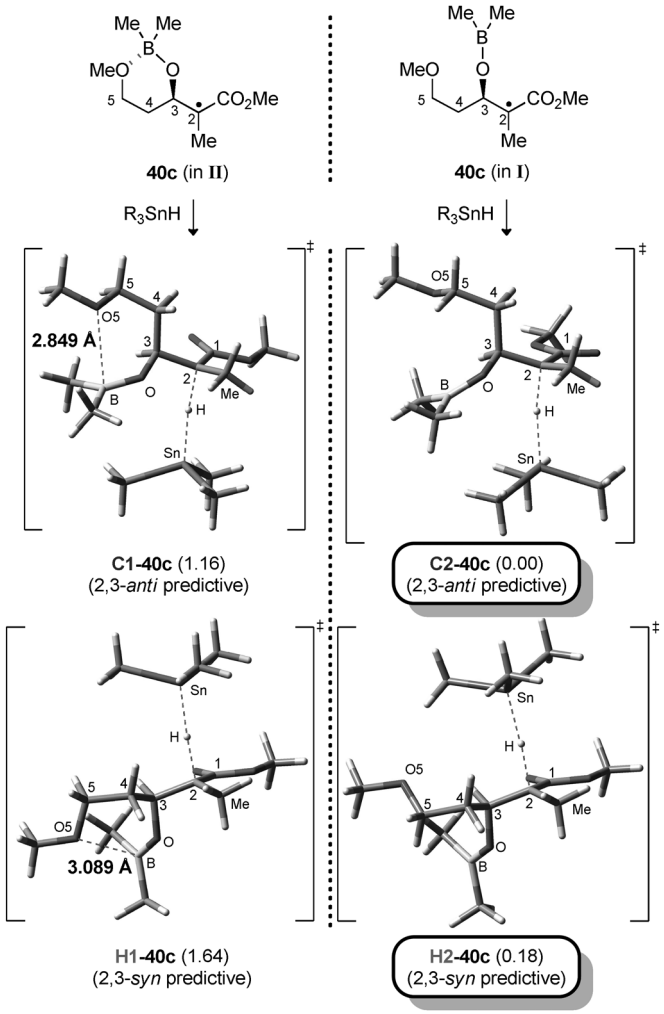

Figure 10. Borinate intermediates **40c** in TS **C** (*anti*-predictive) or **H** (*syn*-predictive) with conformations analogous to **I** or **II** (Figure 8). Energies [kcal mol^{-1}] in DCM are reported relative to the energy of **C2-40c** and B−O5 atomic distances [Å] are shown for the TS structures.

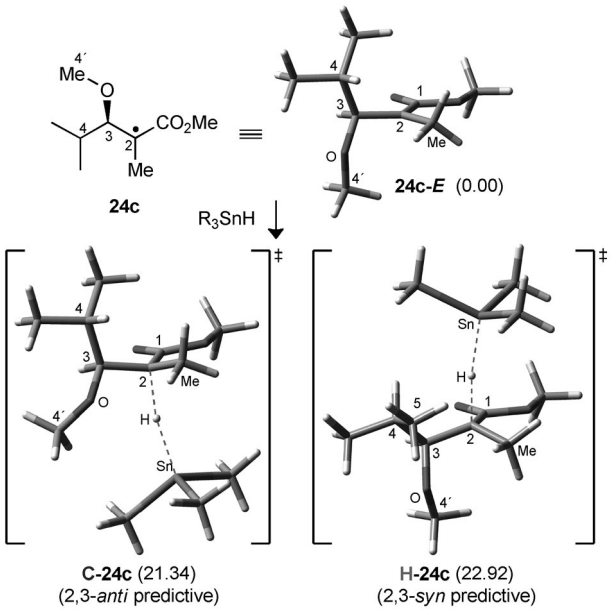

conditions			$\Delta\Delta G^{\ddagger}$ (2,3-*anti* **31a**/2,3-*syn* **31b**)	
hydride	solvent	*T* [°C]	exptl	calcd
Me_3SnH	vacuum	−78	–	**1.73** (>80:1)
Me_3SnH	toluene	−78	–	**1.58** (>50:1)
Bu_3SnH	toluene	−78	**>1.16** (>20:1)	–
Me_3SnH	toluene	25	**1.09** (6.3:1)	–
Bu_3SnH	toluene	25	**1.04** (5.8:1)	–

Figure 11. Transition states of acyclic radical intermediate **24c** (from **24a**,**b**) with a methoxy at C3−O. Gibbs free energies [kcal mol^{-1}] of TS structures in toluene are reported relative to the energy of **24c-*E***.

mains high (1.58 kcal mol^{-1})[35] and correlates with the high selectivity (>20:1) measured experimentally at −78 °C (Figure 11).[44] It can, therefore, be proposed that a bulkier C3 alkyl side chain generates high diastereoselectivity by raising the energy of the *syn*-predictive TS **H**. Various tin hydrides (Me_3SnH and Ph_3SnH) were examined for the reduction of **24c** at 25 °C (Figure 11). As for the reduction of **19c** (Figure 9), Me_3SnH provided selectivities comparable to Bu_3SnH (6.3:1 vs. 5.8:1).

Calculations for borinate radical intermediate **25c** indicated a sufficient $\Delta\Delta G^{\ddagger}$ value to account for the selective formation of the 2,3-*anti* product **32a** (Figure 12). The excellent

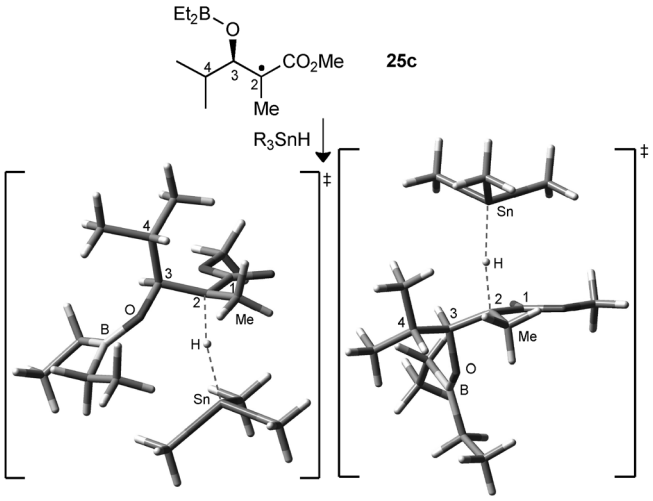

conditions at −78°C	ΔΔG‡ (2,3-*anti* **32a**/2,3-*syn* **32b**)	
	exptl[a]	calcd
vacuum	–	**1.63** (>65:1)
DCM	**>1.16** (>20:1)	**1.59** (>60:1)

[a] Experiments were performed with Bu_3SnH.

Figure 12. Transition states of acyclic radical intermediate **25c** (in situ from **25a**,**b**) with a diethylborinate (BEt_2) at C3−O. Gibbs free energies [kcal mol^{-1}] of TS structures in DCM are reported relative to the energy of **25c**-***E***.

anti-selectivity are rationalized, as for **24c**, by significant destabilizing interaction of *syn*-TS resulting from the presence of a bulky C3-alkyl side chain.[35] It is noteworthy that the borinate and methoxy group adopt conformations in *anti*-predictive TS **C** that remove severe interactions with the incoming hydride. The $\Delta E^{\ddagger}_{strain}$ cost of borinate **25c**, however, is significantly lower than for methoxy **24c** (4.68 vs. 5.80, Figure 13), likely due to pseudo-allylic-1,3 strain ($A^{1,3}$) minimization between the alkyl chain attached to the sp^2 boron and the vicinal C3 stereogenic center in **25c**.[45] Radical **24c** in TS **C** rather presents a fully eclipsed C3−O conformer. The particular conformational bias of borinate group could find application in other reactions in which interactions with an alkoxy-protecting group need to be avoided.

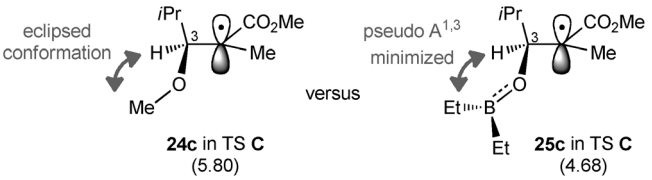

Figure 13. The $\Delta E^{\ddagger}_{strain}$ of radical **24c** versus **25c** in TS **C** (*anti*-predictive). Electronic energies [kcal mol^{-1}] are reported relative to the energies of the respective ground state structures of **24c**-***E*** and **25c**-***E***.

Conclusion

The study of rigid bicyclic 6,7-*trans*-octahydrochromen radical precursors demonstrated the critical impact of positioning the radical-bearing chain equatorial to take advantage of the exocyclic effect. When the radical is forced to occupy an axial position on a THP ring, severe loss of *anti*-selectivity occurs. DFT calculations of TS structures indicate that this phenomenon can be attributed to important interactions between the C2-methyl group and THP ring centers (C5 and C7). Functionalized THP systems, which are expected to impose a bias to the orientation of the radical chain, are under active investigation and will be reported in due course.

The increased conformational energy required for acyclic systems to reach their *anti*-predictive TS explains why they undergo radical reductions with lower selectivities than exocyclic THP. When a tertiary side chain is present at C3, the *syn*-predictive TS are significantly destabilized by additional *syn*-pentane interactions, resulting in a sufficient $\Delta\Delta G^{\ddagger}$ to attain high selectivities. Experimental and computational evidences indicate that high *anti*-selectivities with borinate intermediates are not linked to the formation of a complex mimicking the exocycle. These species prefer to adopt a planar geometry that could facilitate the entry of the incoming hydride in the *anti*-predictive TS.

In summary, this study answers fundamental questions related to the successful reduction of radical substrates. From a more general perspective, the different conformational factors identified herein are likely to influence other reactions taking place at a center vicinal to a heterocycle or an α-alkoxy group.

Experimental Section

Supporting Information: The Supporting Information includes the experimental procedures, physical characterization and NMR spectra (^{1}H and ^{13}C) of radical precursors (**11**–**12a**,**b**, **19**–**23a**,**b**, **25a**,**b**, **33**–**35a**,**b**) and reduced products (**17**–**18a**,**b**, **26**–**30a**,**b**, **32a**,**b**, **37**–**39a**,**b**); and optimized geometries, energies and Cartesian coordinates for all ground and transition states structures.

Computational method for the conformational analysis of radical intermediates: All geometry optimizations were performed using standard gradient techniques and tight SCF convergence in Gaussian 09[15] with the BHandHLYP exchange-correlation (XC) functional[16] using restricted (RBHandHLYP) and unrestricted (UBHandHLYP) methods for closed- and open-shell systems, respectively.[46] It was previously demonstrated[17] that BHandHLYP functional performed better for radical sys-

tems than other XC functionals,[18] disparity often associated with inadequate treatment of the exchange terms.[47] The effective core potential of Hay and Wadt[19] LANL2DZ supplemented with a single set of d-type polarization functions was used for tin ($d(\zeta)Sn = 0.20$)[18b,d,20] together with the valence triple-ζ TZVP basis set[21] for all other atoms. Ground state (GS) radicals were evaluated by unconstrained optimization of all possible rotating bonds including both *E*- and *Z*-enol radical conformations. Staggered transition states (TS) for hydride delivery using Me_3SnH (*anti*- and *syn*-predictive TS) were considered for each conformation of methyl ester radical intermediates. Unscaled harmonic frequency calculations at the appropriate temperature were performed for each optimized structure to characterize it as an energy minimum or a TS structure and to calculate Gibbs free energies ($\Delta G^{\ddagger}$). To calculate Gibbs free energies in solution, geometry optimizations and harmonic frequency calculations were performed with the IEFPCM model[22] and the UFF atomic radii for either toluene or dichloromethane. Wiberg bond indices[48] were calculated using the natural bonding orbitals[49] as implemented in Gaussian 09.[15] The stereochemistry of the radical precursor at C2 was demonstrated experimentally to be unrelated to the stereochemical outcome of radical reduction reaction.[4a,c,d, f] It was thus reasonable to consider the same radical intermediates generated from both halide isomers at the C2 position at the transition state.

Acknowledgements

The authors wish to express their gratitude to the Natural Sciences and Engineering Research Council of Canada (NSERC) for financial support. Fellowship support (B2) from Fonds Québécois de la Recherche sur la Nature et les Technologies (FQRNT) to F.G. is also gratefully acknowledged. We also thank Prof. Tom K. Woo for providing access to the high-performance computing facilities at the University of Ottawa.

[1] a) D. P. Curran, W. Shen, J. C. Zhang, T. A. Heffner, *J. Am. Chem. Soc.* **1990**, *112*, 6738–6740; b) N. A. Porter, I. J. Rosenstein, R. A. Breyer, J. D. Bruhnke, W. X. Wu, A. T. Mcphail, *J. Am. Chem. Soc.* **1992**, *114*, 7664–7676; c) J. G. Stack, D. P. Curran, S. V. Geib, J. Rebek, P. Ballester, *J. Am. Chem. Soc.* **1992**, *114*, 7007–7018; d) M. P. Sibi, J. G. Ji, *Angew. Chem.* **1996**, *108*, 198–200; *Angew. Chem. Int. Ed. Engl.* **1996**, *35*, 190–192; e) M. P. Sibi, J. G. Ji, *J. Org. Chem.* **1996**, *61*, 6090–6091.

[2] a) J. H. Wu, R. Radinov, N. A. Porter, *J. Am. Chem. Soc.* **1995**, *117*, 11029–11030; b) M. Murakata, T. Jono, Y. Mizuno, O. Hoshino, *J. Am. Chem. Soc.* **1997**, *119*, 11713–11714; c) N. A. Porter, J. H. L. Wu, G. R. Zhang, A. D. Reed, *J. Org. Chem.* **1997**, *62*, 6702–6703.

[3] a) D. J. Hart, H. C. Huang, R. Krishnamurthy, T. Schwartz, *J. Am. Chem. Soc.* **1989**, *111*, 7507–7519; b) B. Giese, M. Bulliard, H. G. Zeitz, *Synlett* **1991**, 425–427; c) Y. Guindon, J. F. Lavallée, L. Boisvert, C. Chabot, D. Delorme, C. Yoakim, D. Hall, R. Lemieux, B. Simoneau, *Tetrahedron Lett.* **1991**, *32*, 27–30.

[4] a) Y. Guindon, K. Houde, M. Prévost, B. Cardinal-David, S. R. Landry, B. Daoust, M. Bencheqroun, B. Guérin, *J. Am. Chem. Soc.* **2001**, *123*, 8496–8501; b) Y. Guindon, M. Prévost, P. Mochirian, B. Guérin, *Org. Lett.* **2002**, *4*, 1019–1022; c) P. Mochirian, B. Cardinal-David, B. Guérin, M. Prévost, Y. Guindon, *Tetrahedron Lett.* **2002**, *43*, 7067–7071; d) J.-F. Brazeau, P. Mochirian, M. Prévost, Y. Guindon, *J. Org. Chem.* **2009**, *74*, 64–74; e) J.-F. Brazeau, A. A. Guilbault, J. Kochuparampil, P. Mochirian, Y. Guindon, *Org. Lett.* **2010**, *12*, 36–39; f) P. Mochirian, F. Godin, I. Katsoulis, I. Fontaine, J.-F. Brazeau, Y. Guindon, *J. Org. Chem.* **2011**, *76*, 7654–7676; g) F. Godin, I. Katsoulis, E. Fiola-Masson, S. Dhambri, P. Mochirian, Y. Guindon, *Synthesis* **2012**, *44*, 474–488.

[5] M. M. Faul, B. E. Huff, *Chem. Rev.* **2000**, *100*, 2407–2473.

[6] Four total syntheses of zincophorin (**1a**) have been reported to date: a) S. J. Danishefsky, H. G. Selnick, M. P. Deninno, R. E. Zelle, *J. Am. Chem. Soc.* **1987**, *109*, 1572–1574; b) M. Defosseux, N. Blanchard, C. Meyer, J. Cossy, *J. Org. Chem.* **2004**, *69*, 4626–4647; c) K. Komatsu, K. Tanino, M. Miyashita, *Angew. Chem.* **2004**, *116*, 4441–4445; *Angew. Chem. Int. Ed.* **2004**, *43*, 4341–4345; d) T. J. Harrison, S. Ho, J. L. Leighton, *J. Am. Chem. Soc.* **2011**, *133*, 7308–7311; e) Z. L. Song, A. G. Lohse, R. P. Hsung, *Nat. Prod. Rep.* **2009**, *26*, 560–571; f) G. Sabitha, R. Srinivas, J. S. Yadav, *Synthesis* **2011**, 1484–1488.

[7] a) Y. Kishi, S. Hatakeyama, M. D. Lewis, in *Frontiers of Chemistry* (Ed.: K. J. Laidler), Pergamon, Oxford, **1982**; b) J. A. Tino, M. D. Lewis, Y. Kishi, *Heterocycles* **1987**, *25*, 97–104.

[8] a) Y. Guindon, C. Yoakim, V. Gorys, W. W. Ogilvie, D. Delorme, J. Renaud, G. Robinson, J. F. Lavallée, A. Slassi, G. Jung, J. Rancourt, K. Durkin, D. Liotta, *J. Org. Chem.* **1994**, *59*, 1166–1178; b) Y. Guindon, A. Slassi, J. Rancourt, G. Bantle, M. Bencheqroun, L. Murtagh, E. Ghiro, G. Jung, *J. Org. Chem.* **1995**, *60*, 288–289; c) Y. Guindon, A. M. Faucher, E. Bourque, V. Caron, G. Jung, S. R. Landry, *J. Org. Chem.* **1997**, *62*, 9276–9283; d) Y. Guindon, G. Jung, B. Guérin, W. W. Ogilvie, *Synlett* **1998**, 213–220; e) Y. Guindon, Z. P. Liu, G. Jung, *J. Am. Chem. Soc.* **1997**, *119*, 9289–9290; f) J. P. Bouvier, G. Jung, Z. P. Liu, B. Guérin, Y. Guindon, *Org. Lett.* **2001**, *3*, 1391–1394.

[9] C. H. Schiesser, M. A. Skidmore, *Chem. Commun.* **1996**, 1419–1420.

[10] Y. Guindon, J. Rancourt, *J. Org. Chem.* **1998**, *63*, 6554–6565.

[11] a) E. L. Eliel, N. L. Allinger, S. J. Angyal, G. A. Morrison, *Conformational Analysis*, Wiley, New York, **1965**; b) E. L. Eliel, S. H. Wilen, L. N. Mander, *Stereochemistry of Organic Compounds*, Wiley, New York, **1994**; c) U. Salzner, P. V. Schleyer, *J. Org. Chem.* **1994**, *59*, 2138–2155; d) E. Juaristi, *Conformational Behaviour of Six-Membered Rings*, VCH, Weinheim, **1995**; e) C. W. Beckett, K. S. Pitzer, R. Spitzer, *J. Am. Chem. Soc.* **1947**, *69*, 2488–2495.

[12] Detailed experimental procedures and characterization for all new compounds are reported in the Supporting Information.

[13] a) R. Pappo, D. S. Allen, R. U. Lemieux, W. S. Johnson, *J. Org. Chem.* **1956**, *21*, 478–479; b) W. S. Yu, Y. Mei, Y. Kang, Z. M. Hua, Z. D. Jin, *Org. Lett.* **2004**, *6*, 3217–3219.

[14] a) D. Urankar, I. Rutar, B. Modec, D. Dolenc, *Eur. J. Org. Chem.* **2005**, 2349–2353; b) B. Zajc, *Synth. Commun.* **1999**, *29*, 1779–1784.

[15] Gaussian 09, Revision A.02, M. J. Frisch, G. W. Trucks, H. B. Schlegel, G. E. Scuseria, M. A. Robb, J. R. Cheeseman, G. Scalmani, V. Barone, B. Mennucci, G. A. Petersson, H. Nakatsuji, M. Caricato, X. Li, H. P. Hratchian, A. F. Izmaylov, J. Bloino, G. Zheng, J. L. Sonnenberg, M. Hada, M. Ehara, K. Toyota, R. Fukuda, J. Hasegawa, M. Ishida, T. Nakajima, Y. Honda, O. Kitao, H. Nakai, T. Vreven, J. A. Montgomery, Jr., J. E. Peralta, F. Ogliaro, M. Bearpark, J. J. Heyd, E. Brothers, K. N. Kudin, V. N. Staroverov, R. Kobayashi, J. Normand, K. Raghavachari, A. Rendell, J. C. Burant, S. S. Iyengar, J. Tomasi, M. Cossi, N. Rega, J. M. Millam, M. Klene, J. E. Knox, J. B. Cross, V. Bakken, C. Adamo, J. Jaramillo, R. Gomperts, R. E. Stratmann, O. Yazyev, A. J. Austin, R. Cammi, C. Pomelli, J. W. Ochterski, R. L. Martin, K. Morokuma, V. G. Zakrzewski, G. A. Voth, P. Salvador, J. J. Dannenberg, S. Dapprich, A. D. Daniels, Ö. Farkas, J. B. Foresman, J. V. Ortiz, J. Cioslowski, D. J. Fox, Gaussian, Inc., Wallingford, CT, **2009**.

[16] BHandHLYP functional is a hybrid functional defined as a half-and-half combination of HF and Becke exchange with Lee–Yang–Parr correlation functional: $0.5 \times E_X^{HF} + 0.5 \times E_X^{LSDA} + 0.5 \times \Delta E_X^{Becke88} + E_C^{LYP}$ (Gaussian 09).

[17] M. Mohr, H. Zipse, D. Marx, M. Parrinello, *J. Phys. Chem. A* **1997**, *101*, 8942–8948.

[18] a) T. Morihovitis, C. H. Schiesser, M. A. Skidmore, *J. Chem. Soc. Perkin Trans. 2* **1999**, 2041–2047; b) H. Matsubara, C. H. Schiesser, *Org. Biomol. Chem.* **2003**, *1*, 4335–4341; c) H. Matsubara, C. T. Falzon, I. Ryu, C. H. Schiesser, *Org. Biomol. Chem.* **2006**, *4*, 1920–1926; d) H. Matsubara, I. Ryu, C. H. Schiesser, *J. Org. Chem.* **2005**, *70*, 3610–3617; e) H. Matsubara, I. Ryu, C. H. Schiesser, *Org. Biomol. Chem.* **2007**, *5*, 3320–3324; f) S. H. Kyne, C. H. Schiesser, H. Matsubara, *Org. Biomol. Chem.* **2007**, *5*, 3938–3943; g) S. H. Kyne, C. H. Schiesser, H. Matsubara, *J. Org. Chem.* **2008**, *73*, 427–434.

[19] W. R. Wadt, P. J. Hay, *J. Chem. Phys.* **1985**, *82*, 284–298.
[20] R. Nakayama, H. Matsubara, D. Fujino, T. Kobatake, S. Yoshida, H. Yorimitsu, K. Oshima, *Org. Lett.* **2010**, *12*, 5748–5751.
[21] A. Schäfer, C. Huber, R. Ahlrichs, *J. Chem. Phys.* **1994**, *100*, 5829–5835.
[22] M. Cossi, G. Scalmani, N. Rega, V. Barone, *J. Chem. Phys.* **2002**, *117*, 43–54.
[23] J. I. Seeman, *Chem. Rev.* **1983**, *83*, 83–134.
[24] a) L. M. Wu, H. Fischer, *Helv. Chim. Acta* **1983**, *66*, 1588; b) B. Giese, W. Damm, F. Wetterich, H. G. Zeitz, *Tetrahedron Lett.* **1992**, *33*, 1863–1866; c) B. Giese, W. Damm, F. Wetterich, H. G. Zeitz, J. Rancourt, Y. Guindon, *Tetrahedron Lett.* **1993**, *34*, 5885–5888.
[25] M. D. Fernández-Alonso, J. Canada, J. Jimenez-Barbero, G. Cuevas, *ChemPhysChem* **2005**, *6*, 671–680.
[26] This transition state energy was determined to be the lowest for substrate **2c** calculated with Me_3SnH using BHandHLYP/TZVP level of theory.
[27] Modeling was performed on methyl ester analogue of **2**.
[28] All these transition states (*anti*- and *syn*-predictive TS) were considered for hydride delivery using Me_3SnH for each conformation (*E* and *Z*) of methyl ester radical intermediates.
[29] G. S. Hammond, *J. Am. Chem. Soc.* **1955**, *77*, 334–338.
[30] This angle was determined from the plane formed by C3-C1-C2 and C2–C3.
[31] The reduced products were pyramidalized to nearly 18° at C3 in the ground state.
[32] Y. Guindon, C. Yoakim, R. Lemieux, L. Boisvert, D. Delorme, J. F. Lavallée, *Tetrahedron Lett.* **1990**, *31*, 2845–2848.
[33] The following nomenclature was used throughout the manuscript: TS-radical intermediate-orientation. For example, **C-2c-eq** corresponds to radical intermediate **2c** in the conformation of TS C while oriented equatorially (eq).
[34] J. M. Lee, P. Helquist, O. Wiest, *J. Am. Chem. Soc.* **2012**, *134*, 14973–14981.
[35] See the Supporting Information for details.
[36] D. A. Evans, V. J. Cee, S. J. Siska, *J. Am. Chem. Soc.* **2006**, *128*, 9433–9441.
[37] a) F. M. Bickelhaupt, *J. Comput. Chem.* **1999**, *20*, 114–128; b) A. Diefenbach, F. M. Bickelhaupt, *J. Chem. Phys.* **2001**, *115*, 4030–4040; c) A. Diefenbach, F. M. Bickelhaupt, *J. Phys. Chem. A* **2004**, *108*, 8460–8466; d) A. Diefenbach, G. T. de Jong, F. M. Bickelhaupt, *J. Chem. Theory Comput.* **2005**, *1*, 286–298; e) G. T. de Jong, F. M. Bickelhaupt, *ChemPhysChem* **2007**, *8*, 1170–1181; f) A. P. Bento, F. M. Bickelhaupt, *J. Org. Chem.* **2008**, *73*, 7290–7299; g) I. Fernández, F. M. Bickelhaupt, F. P. Cossio, *Chem. Eur. J.* **2009**, *15*, 13022–13032; h) W. J. van Zeist, F. M. Bickelhaupt, *Org. Biomol. Chem.* **2010**, *8*, 3118–3127.
[38] a) C. Y. Legault, Y. Garcia, C. A. Merlic, K. N. Houk, *J. Am. Chem. Soc.* **2007**, *129*, 12664–12665; b) D. H. Ess, K. N. Houk, *J. Am. Chem. Soc.* **2008**, *130*, 10187–10198; c) S. I. Gorelsky, D. Lapointe, K. Fagnou, *J. Am. Chem. Soc.* **2008**, *130*, 10848–10849; d) C. B. Shinisha, R. B. Sunoj, *J. Am. Chem. Soc.* **2010**, *132*, 12319–12330.
[39] B. Guérin, C. Chabot, N. Mackintosh, W. W. Ogilvie, Y. Guindon, *Can. J. Chem.* **2000**, *78*, 852–867.
[40] a) G. E. Keck, S. Castellino, *Tetrahedron Lett.* **1987**, *28*, 281–284; b) D. A. Evans, B. D. Allison, M. G. Yang, C. E. Masse, *J. Am. Chem. Soc.* **2001**, *123*, 10840–10852.
[41] S. Kiyooka, M. Shiinoki, K. Nakata, F. Goto, *Tetrahedron Lett.* **2002**, *43*, 5377–5380.
[42] M. Drouin, A. G. Michel, Y. Guindon, W. Ogilvie, *Acta Crystallogr. Sect. C* **1993**, *49*, 75–77.
[43] a) A. E. Finholt, A. C. Bond, K. E. Wilzbach, H. I. Schlesinger, *J. Am. Chem. Soc.* **1947**, *69*, 2692–2696; b) R. H. Fish, H. G. Kuivila, I. J. Tyminski, *J. Am. Chem. Soc.* **1967**, *89*, 5861–5868.
[44] Y. Guindon, B. Guérin, J. Rancourt, C. Chabot, N. Mackintosh, W. W. Ogilvie, *Pure Appl. Chem.* **1996**, *68*, 89–96.
[45] The strain energy of the hydride ($\Delta E^{\neq}_{strain}$ [hydride]) and the interaction energy ($\Delta E^{\neq}_{int}$) were found to be marginally different in these two systems. See the Supporting Information for details.
[46] W. J. Hehre, L. Radom, P. v. R. Schleyer, P. A. Pople, *Ab Initio Molecular Orbital Theory*, Wiley, New York, **1986**.
[47] V. Tschinke, T. Ziegler, *Theor. Chim. Acta* **1991**, *81*, 65–78.
[48] K. B. Wiberg, *Tetrahedron* **1968**, *24*, 1083–1096.
[49] E. D. Glendening, A. E. Reed, J. E. Carpenter, F. Weinhold, Theoretical Chemistry Institute and Department of Chemistry, University of Wisconsin, Madison, WI.

Received: January 30, 2013
Published online: June 3, 2013

